

Hydrogen Ionization Inside the Sun

Vladimir A. Baturin¹ · Sergey V. Ayukov¹ · Anna V. Oreshina¹ · Alexey B. Gorshkov¹ · Victor K. Gryaznov² · Igor L. Iosilevskiy^{3,4} · Werner Däppen⁵

© The author(s)

Abstract Hydrogen is the main chemical component of the solar plasma, and H-ionization determines basic properties of the first adiabatic exponent Γ_1 . Hydrogen ionization remarkably differs from the ionization of other chemicals. Due to the large number concentration, H-ionization causes a very deep lowering of Γ_1 , and the lowering profile appears to be strongly asymmetric and extends over almost the entire solar convective zone. The excited states in the hydrogen atom are modelled with the help of a partition function, which accounts the internal degrees of freedom of the composed particle. A temperature-dependent partition function with an asymptotic cut-off tail is deduced from a solution of the quantum mechanical problem of the hydrogen atom in the plasma. We present a numerical simulation of hydrogen ionization, calculated with two expressions for the partition function, Planck-Larkin (PL) and Starostin-Roerich (SR), respectively. The Hydrogen ionization is shifted toward higher temperature in the SR-case compared to the PL-case. Different models for excited states of the hydrogen atom may change Γ_1 by as much as 10^{-2} . The behavior of the Γ_1 profiles for pure hydrogen resembles “twisted ropes” for the two considered models. This significantly affects the helium ionization and the position of the helium hump. This entanglement of H and He effect gives us a chance to study a role of excited states in the solar plasma.

✉ A.V.Oreshina
avo@sai.msu.ru

- ¹ Sternberg Astronomical Institute, M.V. Lomonosov Moscow State University, Moscow, Russia
- ² Federal Research Center of Problems of Chemical Physics and Medicinal Chemistry RAS, Chernogolovka, Russia
- ³ Joint Institute for High Temperatures RAS, Moscow, Russia
- ⁴ Moscow Institute of Physics and Technology, Dolgoprudnyi, Russia
- ⁵ Department of Physics and Astronomy, University of Southern California, Los Angeles, CA 90089, USA

Keywords: Plasma Physics; Interior, Convective Zone; Helioseismology, Direct Modeling

1. Introduction

The equation of state (EOS) is a key element in the modeling of the solar structure. Its role is especially obvious in the problem of helioseismic inverse modeling to restore physical features of the solar plasma. The equation of state is used to compute measurable thermodynamic functions (pressure, adiabatic exponent, specific heat capacity, etc.) for given temperature, density, and chemical composition of equilibrium plasma.

The most striking and obvious physical effect in the theory of the EOS under solar conditions is the ionization of elements, among which hydrogen and helium give the strongest effect both in terms of pressure P and adiabatic exponent Γ_1 , describing elasticity of the plasma. Γ_1 is variation of pressure under adiabatic compression: $\Gamma_1 = \partial \ln P / \partial \ln \rho|_S$. We consider how ionization affects the adiabatic exponent, calculated along some fixed sequence of points (T, ρ) of a standard solar model. For illustration, examples of Γ_1 profiles are shown in Figure 1. The red curve shows the Γ_1 profile for a purely hydrogen plasma, while the blue curve shows the Γ_1 profile for a plasma composed of hydrogen and helium, with mass contents of hydrogen $X = 0.75$ and helium $Y = 0.25$, which is close to the solar content.

The ionization of hydrogen is strikingly different from that of other elements. First, due to the abundance of hydrogen (90% in number of particles), the decrease of Γ_1 in the ionization region turns out to be very strong and the value of Γ_1 falls from values around $5/3$ to 1.2. Secondly, the ionization of hydrogen occurs against the background of an almost complete absence of free electrons from other ions. Therefore, mainly electrons from the ionization of hydrogen itself must be taken into account. This leads to the fact that the initial ionization of hydrogen occurs very abruptly and at very low temperatures compared to the ionization energy, i.e. $I_H/kT > 10$. Here I_H is the ionization energy of the hydrogen atom from the ground state, and k is the Boltzmann constant. The decrease of Γ_1 occurs almost by a jump, whereas the subsequent transition of the curve to full ionization extends over a significant area in depth, up to temperatures $I_H/kT < 1$, which extends over a significant part of the convective zone

Thus, an accurate calculation of the Γ_1 profile in the hydrogen ionization region is a difficult task. The question of the equation of state of hydrogen in a wide range of conditions has been considered in many works in the physical literature. The most advanced approaches were considered by Militzer and Ceperley (2001); Militzer and Hubbard (2013); Wendland, Ballenegger, and Alastuey (2014); Chabrier, Mazevet, and Soubiran (2019); Chabrier and Debras (2021); Filinov and Bonitz (2023). But we do not know application of these results to solar modeling. In the astrophysical application for modeling stars, the following EOS calculations are known: Mihalas, Däppen, and Hummer (1988);

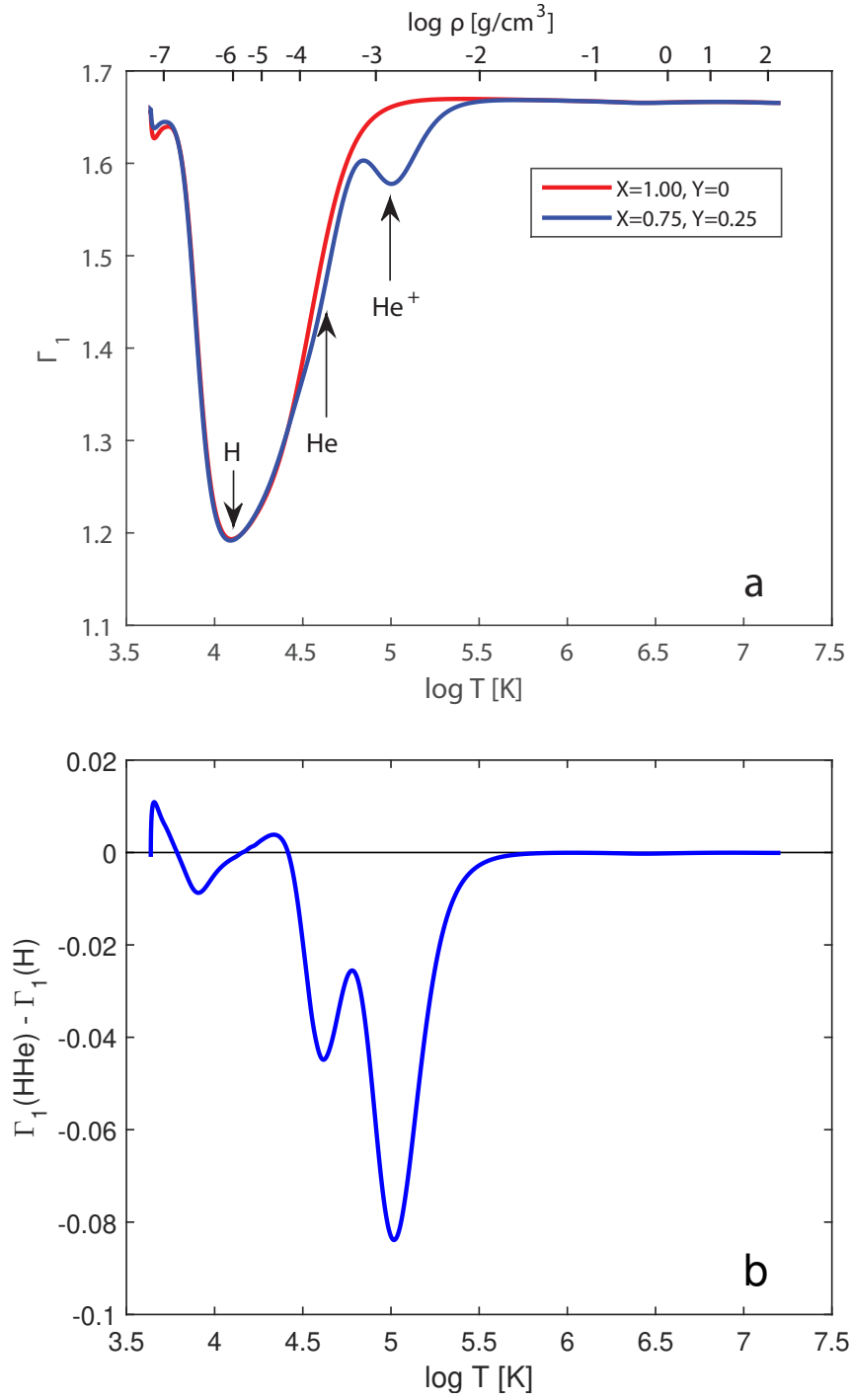


Figure 1. (a) Adiabatic exponent profiles for hydrogen (*red curve*) and hydrogen-helium (*blue curve*) plasmas calculated at points (T, ρ) from the standard solar model. (b) Difference between Γ_1 of hydrogen-helium and hydrogen plasma.

Rogers, Swenson, and Iglesias (1996); Rogers and Nayfonov (2002); Irwin (2012). Appendix A presents comparison of Γ_1 for available equations of state.

The main problem is related to the modeling the quantum structure of the hydrogen atom under conditions of sufficiently large density and high plasma temperatures. In other words, while the isolated hydrogen atom is a well-studied problem with known quantum states and statistical weights, in a plasma, the hydrogen atom is a difficult system due to the presence of nearby other particles with sufficiently high kinetic energy.

The example of the ionization of pure hydrogen is quite far from the real conditions on the Sun. To approximate reality, we demonstrate also the role of helium ionization against the background of completed hydrogen ionization. Due to the larger first ionization potential, helium is ionized at higher temperatures than hydrogen, and the ratio to the ionization potential turns out to be $I_{He}/kT > 7$. The difficulty in ionization of helium is due to the fact that abundant free electrons from significantly ionized hydrogen are present. The lower panel of Figure 1 shows the difference in Γ_1 when helium is present compared to pure hydrogen. This difference serves as a qualitative estimate of the He contribution. Note that the He contribution generally resembles the theory of Z contributions for He-like heavy element ions discussed in (Baturin et al. 2022). It also follows from this figure that the first helium ionization leads to a lowering of the Γ_1 profile by about 0.05 at $\log T = 4.55$, while the second ionization lowers Γ_1 by about 0.09 at $\log T = 5$.

The issue of theoretical modeling of the ‘ionization glitch’ for helium ionization is discussed by Houdayer et al. (2021).

We focus on solving a restricted problem of changing the profile of adiabatic exponent Γ_1 due to perturbation of the effective statistical weight of hydrogen in a narrow region inside the Sun, where transition from a neutral composition to a fully ionized state occurs. Hydrogen ionization occurs inside the Sun and in solar-type stars in the outermost envelope at relatively low temperature $T \sim 10^4 - 10^5$ K. The density of the plasma is also quite low, $\rho \sim 10^{-7} - 10^{-3}$ g cm $^{-3}$.

The issues of hydrogen ionization beyond solar-like stars, for example in low-mass stars and planets, as well as the asymptotic behavior at high density and/or temperature regimes are outside the scope of this paper.

The key object of our study is the so-called Planck-Larkin (PL) partition function. The history of the partition function goes back to one hundred years ago to work by Planck (1924). This story is described in excellent details by W. Ebeling in historical essay (Ebeling 2017). Although the partition function formula was originally written by Brillouin (1930) it is commonly referred to as the Planck-Larkin partition function under which name it was essentially rediscovered in the framework of “field-theoretical statistical thermodynamics by Vedenov and Larkin, 1960” (cited from Ebeling 2017; original papers are Vedenov and Larkin 1959; Larkin 1960). The further development of theory may be found in a series of papers by Ebeling, the most recent is Ebeling, Reinholz, and Röpke (2021).

We fix all the internal parameters of an EOS model, except of the partition function (PF hereafter). In particular, we keep the model of Coulomb interaction

which is noticeable in the studied area. Moreover, there are many other assumptions: the degeneracy and relativism of electrons, the presence of molecules and negative ions and others. They are small and not discussed in the paper.

Our work was performed using SAHA-S EOS (Gryaznov et al. 2004, 2006, see also SAHA-S website crydee.sai.msu.ru/SAHA-S.EOS). SAHA-S EOS was created specifically for the analysis of thermodynamics at the conditions of the Sun and solar-type stars. It focuses on those phenomena that are significant in the solar interior, leaving aside extreme domains of very high densities and/or very high temperatures. The basic thermodynamic quantities are computed with high numerical stability that provides smooth profiles of thermodynamic derivatives, including Γ_1 . Some results on this issue can be found in Baturin et al. (2019). The numerical stability in calculating the pressure in SAHA-S is at the level of 10^{-8} , and the stability of calculating derivatives is at the level of 10^{-6} . This is important for the study of sophisticated physical effects and comparison between EOS models at the accuracy level necessary for helioseismic analysis.

2. Ionization Modeling

Ionization simulations are carried out within the framework of the chemical picture. The chemical picture is based on the minimization of the free energy $F(T, V)$ as a function of the concentrations of particles of different varieties: atoms, electrons, and protons in the case of hydrogen plasma at fixed T and V (Harris, Roberts, and Trulio 1960; Ebeling 1969; Graboske, Harwood, and Rogers 1969). These concentrations can be found from additional Saha's ionization equilibrium equations (Saha 1921). The Saha equations are relations for the chemical potentials μ_i of the corresponding ions. For example, for the ionization of hydrogen $H \leftrightarrow p + e^-$, the equation is written as

$$\mu_H - \mu_p - \mu_e = 0 \quad (1)$$

(Prigogine and Defay 1954). In the case of classical (nondegenerate, noninteracted) particles, from Equation 1 the usual form of the Saha equation is obtained, which assumes the existence of the hydrogen atom only in the ground state:

$$\frac{n_p n_e}{n_H} = \frac{g_p g_e}{g_H} \lambda_e^{-3} e^{-I_H/kT}, \quad \lambda_e = \left(\frac{2\pi m_e kT}{h^2} \right)^{1/2}. \quad (2)$$

In this expression n_H , n_p , n_e are concentrations of neutral hydrogen, protons, and free electrons respectively. The variables g_H , g_p , g_e are the statistical weights of the particles, i.e. the parameters describing the internal degree of freedom of the particle. In the case under consideration, $g_p = 1$, $g_e = 2$, $g_H = 2$, while I_H is the ionization potential for the ground state. The value λ_e defined through the classical constants is sometimes called the thermal wavelength of the electron.

However, if we want to take into account the existence of hydrogen not only in the ground state, but also in the excited states, the equation of Saha (2) can

be rewritten as

$$\frac{n_H}{n_e n_p} = \lambda_e^3 \cdot e^{\beta I_H} \sum_{n=1}^{\infty} \tilde{g}_n e^{-\beta \varepsilon_n} w_n. \quad (3)$$

In this case, the excited states are combined in the sum. The notation for the inverse temperature $\beta = (kT)^{-1}$ is introduced. The excitation energies ε_n of each state are equal to $\varepsilon_n = I_H (1 - n^{-2})$. The statistical weight of an individual state in the sum in the formula 3 is modified according to the expression $\tilde{g}_n = g_n / (g_p g_e)$, where $g_n = 2n^2$, and $\tilde{g}_n = n^2$. The main feature in the new Equation 3 are weight cut-off factors w_n , which describe the possibility of existence of hydrogen states with high quantum numbers n in a high-temperature dense plasma.

Choosing a system of weight functions w_n is one of the most difficult problems in modeling of dense plasmas. One advanced solution was implemented in the MHD EOS (Mihalas, Däppen, and Hummer 1988). In this paper we estimate the partition function as it was proposed in the SAHA-S EOS framework (Gryaznov et al. 2004, 2006).

Before moving on to the properties and calculations of cut-off factors and the sum over excited states, let us point out the reason why we cannot do without them. Assuming $w_n = 1$, for all n , several problems arise. On the one hand, summing over infinite number of states in Equation 3 results in a divergent sum at all temperatures, including low temperatures. That is, such a model cannot be used even in the trivial case of neutral hydrogen. On the other hand, if we restrict the sum to any finite number of states, then, as the temperature and density increases toward the center of the Sun, we obtain a prediction of a significant number of neutral hydrogen atoms in the center.

To obtain an alternative set of weight cut-off factors, we use the result obtained in different thermodynamic approach, the framework of the physical picture. In this case, we obtain an expression similar to Equation 3, and equivalent to the law of acting masses (Ebeling, Kraeft, and Kremp 1976). According to this law, the concentration ratio is equal to a function of temperature:

$$\frac{n_H}{n_e n_p} = \lambda_e^3 \cdot U. \quad (4)$$

The function $U(T)$ will be called partition function (hereafter PF):

$$U = e^{\beta I_H} \sum_{n=1}^{\infty} \tilde{g}_n e^{-\beta \varepsilon_n} w_n. \quad (5)$$

In this expression, we denote the sum over quantum states of hydrogen as Q :

$$Q = \sum_{n=1}^{\infty} \tilde{g}_n e^{-\beta \varepsilon_n} w_n. \quad (6)$$

The sum Q is introduced in analogy with the Saha equation (3) and can be interpreted as the effective statistical weight of hydrogen taking into account excited states.

Theoretical solutions have been obtained for the PF in the case of the hydrogen atom, two of which we will use in analyzing the equations of state. One of them is the Planck-Larkin (PL) and the other the Starostin-Roerich (SR) partition functions. They are defined in the next section.

Note that the analogy between the PF and the right part of the Saha equation (3) is superficial and based on external similarity of the obtained expressions. The PF is a result of elaborate quantum-statistical calculations. It is an integral over all possible states of the proton-electron pair, including not only classical hydrogen states, but also so-called scattered states. Expressions in the form of a sum over hydrogen states are only one possible form for PF. But in our case, we take advantage of this analogy and use the expressions of the weight factors w_n from this function to obtain the corresponding expressions in the Saha equation.

It may seem that the sum (6) allows us to determine the populations of excited states. Potekhin (1996) discussed the difference between thermodynamic populations and those observed in optical experiments. In our case, following Rogers (1986), in the low-density limit, using PL partition function, formal thermodynamic populations are given by the formula

$$\frac{n_H^{(n)}}{n_H} = \frac{\tilde{g}_n e^{-\beta \varepsilon_n} w_n}{\sum_{n=1}^{\infty} \tilde{g}_n e^{-\beta \varepsilon_n} w_n}. \quad (7)$$

Rogers (1986) also notes that the populations obtained in this way may differ markedly from the observed (optical) ones, which probably does not allow direct comparison with the populations estimated by Pradhan (2024).

We should prevent from interpretation of the individual terms in the sum of Equation 6 as the populations of a separate excited state. Each term in Equation 6 is the sum of the contributions of bounded and free states (for more details, see Rogers 1986). Only whole sum has the physical meaning and the corresponding cut-off factors provide its convergence.

3. Properties of Cut-off Factors and Partition Function

The purpose of using cut-off factors is to obtain a finite sum in Equation 6 over an infinite number of excited states of hydrogen. It is important that the PF be a differentiable function of temperature, i.e., free of jumps and discontinuities.

The calculations are based on the key function w_n . This function is only a function of temperature, i.e., it does not depend on the density and concentration of particles. To calculate w_n , one also needs the ionization potentials of excited states I_n , which are equal to $I_n = I_H/n^2$ for hydrogen. But ultimately the cut-off factors $w(\alpha)$ are a universal function of a single argument $\alpha = I_n/(kT)$.

The Planck-Larkin partition function discussed in the introduction (commonly, and hereafter named PL) is widely used in the physical literature, for example Ebeling, Kraeft, and Kremp 1976; Krasnikov 1968; Kraeft et al. 1986; Rogers, Swenson, and Iglesias 1996, etc. The definition for the PL cut-off is

$$w_n^{\text{PL}}(\alpha) = 1 - e^{-\beta I_n} - \beta I_n e^{-\beta I_n}. \quad (8)$$

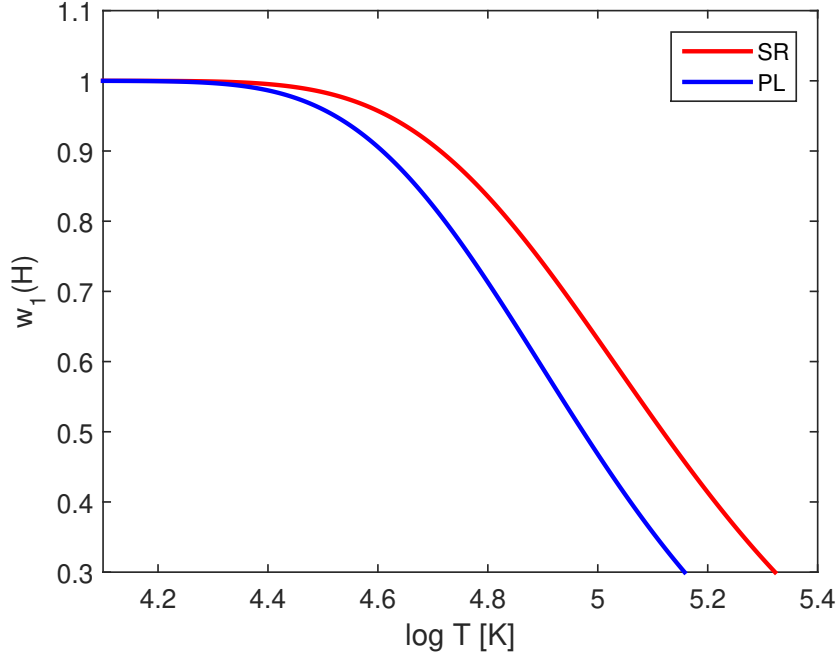


Figure 2. Cutoff factor w_1 for the ground state ($n = 1$) of hydrogen in the PL and SR approximation.

According to Ebeling, Fortov, and Filinov (2017) and Starostin et al. (2009), the PL function partially includes scattered states besides bound states of an atom. Another form of a cut-off factor is introduced in Starostin, Roerich, and More (2003); Starostin and Roerich (2006) which we name SR (after Starostin and Roerich). The SR cutoff factor w_n is more complex than that of PL. It does not include scattered states. The SR partition function is used in SAHA-S equation of state (Gryaznov et al. 2006):

$$w_n^{\text{SR}}(\alpha) = 1 - e^{-\beta I_n} \left[4 - \frac{6}{\sqrt{\pi}} (\beta I_n)^{1/2} + \frac{4}{\sqrt{\pi}} (\beta I_n)^{3/2} \right] + \frac{\Gamma\left(\frac{1}{2}, \beta I_n\right)}{\sqrt{\pi}} \left[3 - 4\beta I_n + 4(\beta I_n)^2 \right]. \quad (9)$$

Here the incomplete gamma function is

$$\Gamma\left(\frac{1}{2}, z\right) = \int_z^{\infty} \frac{e^{-t}}{\sqrt{t}} dt. \quad (10)$$

Formally, the given definitions are sufficient for solving the hydrogen ionization problem. In the following, we will consider the behavior of functions and discuss the difference in the results obtained.

The general behavior of the cut-off factors is shown in Figure 2. Here, the factors are presented as functions of temperature, assuming that the ionization potential is equal to I_H , i.e., for the ground state of hydrogen. This figure is a universal description of cut-off factors. That is, to obtain multipliers for states with the number n , we only have to shift the value of the argument α of the function $w(\alpha)$, assuming that the ionization potential of the excited state is smaller. An example of calculation of the corresponding w_n at one temperature is given in the Appendix B, Figure 8.

The general behavior of the cut-off factors is quite simple. At low temperatures (high values of α), $w = 1$. That is, at the temperature $T = 1.5 \cdot 10^4$ K the factor for the ground state is 1, and makes no contribution to the ionization equation. As the temperature increases, w starts to decrease, and the rate of decrease is asymptotically the same for both functions and is large enough to ensure convergence of the sum. The difference in the two models is that the magnitude of the ratio $w^{\text{SR}}/w^{\text{PL}} \rightarrow 4$ in the limit of high temperatures (Starostin and Roerich 2004). Accordingly, the transition to the region of decrease in the case of the SR model occurs later than in the case of PL. As a result, the $w^{\text{SR}} > w^{\text{PL}}$ and SR multiplier for any state turns out to be always larger than for PL (Figure 2). On the other hand, the ratio of functions $w^{\text{SR}}/w^{\text{PL}}$ varies from unity at low temperatures, to 4 at high temperatures (Gryaznov et al. 2004). This means that at the low temperatures one should not expect a difference in calculations with different models.

Let us return to the question about the factors w for the excited states. States with high n and small ionization potential $I_n = I_H/n^2$ at any temperature will fall into the region of the decreasing tail of the cut-off factors, i.e., will cease to contribute to the sum over states. The only difference is in the value n^* , after which the excited states become negligibly small. At low temperatures, states with $n < n^*$ (excluding the ground state) appear uninhabited due to the Boltzmann factor $e^{-\beta\epsilon_n}$, and higher states with $n > n^*$ are cut off by w . As a result, the whole sum is determined only by the ground state $n = 1$. This effect can be called “freezing” of excited states.

However, as the temperature increases, w_n of all states, including the ground state, decrease. The specificity of the cutoff factors model is that all states start to vanish very early, at low temperatures, but the dependence on n is rather weak. As a result, the most important is the transition region from temperatures where $w = 1$ to the region where all states, including the ground state, are cut off. For the SR function, this transition region is shifted toward high temperatures. As a result, taking into account excited states, the SR model predicts a noticeably higher weight of neutral hydrogen compared to the PL case. Moreover, this increase in the fraction of states is associated precisely with excited states. The contribution of individual states with small n can be seen in Figure 9 in the Appendix B.

Note that the choice of cut-off factors guarantees the exclusion of highly excited states, but it happens as delicately as possible. That is, the cut-off factor behaves with temperature in such a way as to ensure convergence of the sum. In reality, the exclusion of highly excited states can occur more quickly.

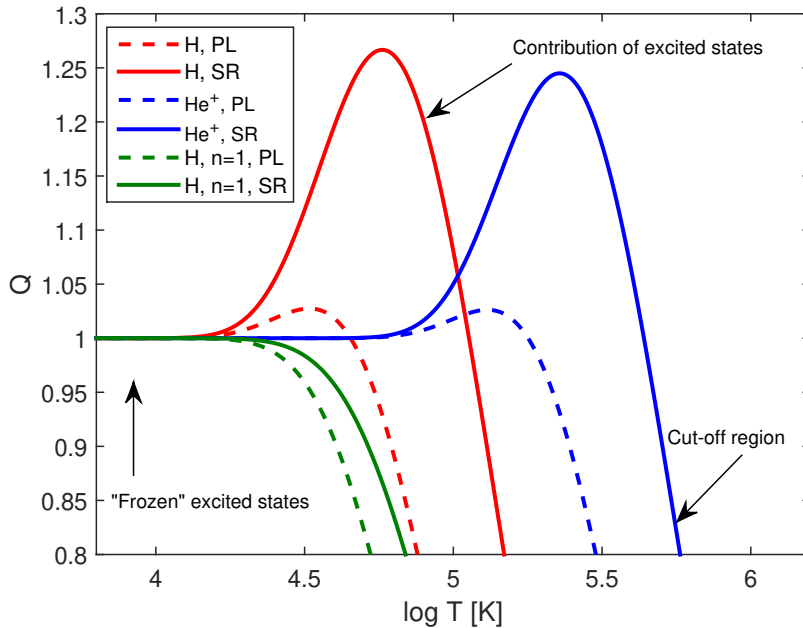


Figure 3. Partition function Q calculated in SAHA-S EOS for hydrogen (*red curves*) and helium (*blue curves*). *Green curves* show contribution of the main state ($n = 1$) of hydrogen atom. *Solid curves* are for SR approach, *dashed* – for PL.

Let us proceed to the calculation of the sum Q (Equation 6) by states using the SR and PL functions. An example of such a calculation is shown in Figure 3.

The terms in the sum (6) are the product of the functions w_n and the Boltzmann multiplier $e^{-\beta\varepsilon_n}$. The behavior of the sum Q depends on where the transition to the cutoff region occurs. It is this region and ionization in it that will be the subject of our consideration.

For each state, w_n only decreases with increasing temperature, but the total sum and PF of hydrogen can grow, reaching a maximum in the intermediate region. This effect is observed even with PL, albeit to a lesser extent, and even more so with SR (see Figure 3).

Hydrogen ionization starts at low temperatures and high values of $\beta I_H \sim 10$. Under these conditions, the difference between w_{PL} and w_{SR} is still minor, since both functions are equal to unity. However, as the temperature increases, the functions show a significant difference between the descriptions within the different models.

The maximum of Q_H^{SR} is 1.25 compared to the maximum of Q_H^{PL} around 1.05. The maximum of Q_H^{SR} is noticeably shifted towards higher temperatures. The SR-function is always larger than the PL-function $Q_H^{SR} > Q_H^{PL}$. Note that the cut-off functions PL or SR have been originally proposed for hydrogen. However they can also be applied to hydrogen-like ions. On the figure 3, the Q -profile for He^+ are shown. In sense of $Q(\alpha)$, the partition function should be the same for all hydrogen-like ions.

In the general case, the cut-off factors do not guarantee absence of inverse recombination of hydrogen because they depend on temperature only. Saha equation with these factors predicts hydrogen becomes neutral while density increases at any fixed temperature.

But we checked the ionization of hydrogen at the center of the Sun. PFs predict the disappearance with temperature of all states, including the ground state. As the temperature increases in the central regions of the Sun, w predicts rather small weights for the ground and other hydrogen states, since the argument α there is equal to 0.01. As a result, the fraction of neutral hydrogen below the convection zone is small. Appendix C shows fraction of hydrogen atoms in the central part of the Sun for the both cases PL and SR.

On the other hand, density effect and limitation of number of levels could affect the calculation of partition function. In Appendix D, we demonstrate the partition function with finite number of levels by applying the Mott condition (see, for example, Ebeling, Kraeft, and Röpke 2012; Ebeling, Reinholz, and Röpke 2020). The effect is insignificant compared to the difference between the PL and SR functions under solar conditions.

The magnitude of the sum Q can be interpreted as the effective statistical weight in the Saha equation (4). Thus, having the calculation of the sum Q in both models, we can proceed to the analysis of hydrogen ionization calculated within the SAHA-S equation.

4. Hydrogen Ionization in Solar Conditions: Results of Calculation

Figure 4 demonstrates hydrogen and helium ionization calculated at the (T, ρ) points of the solar model. Ionization is shifted towards higher temperature in SR-case in comparison with PL-case. Hydrogen ionization in PL-case is systematically larger than SR-case and the difference (red solid line in Figure 4(b)) has the same sign at all temperatures. There are no differences between PFs at low temperatures ($\log T < 4.2$); Q sum equals 1 for both PFs. At higher temperature, the ionization difference is slowly going to zero because both models predict complete ionization here. The difference in hydrogen ionization is remarkable over helium ionization zone with $\log T \simeq 5$. It will cause significant effect on helium hump (see below).

In Figure 4, the helium ionization is also shown. The helium ionization is considered both in PL and SR-model. Generally, the helium ionization differences are similar to those of hydrogen ionization, but fine details in Figure 4(b) look specific for two-electrons ionization. We should note that there is no rigorous background for application of the PL and the SR expressions to the He atom. But in absence of convergent partition function for helium atom, in present SAHA-S calculations, the same form was used for all atomic components.

5. The First Adiabatic Exponent Profile

Figure 5 shows effect of the PF on Γ_1 profiles for pure hydrogen plasma. The profile in the PL case appears to be shifted toward higher temperature at the

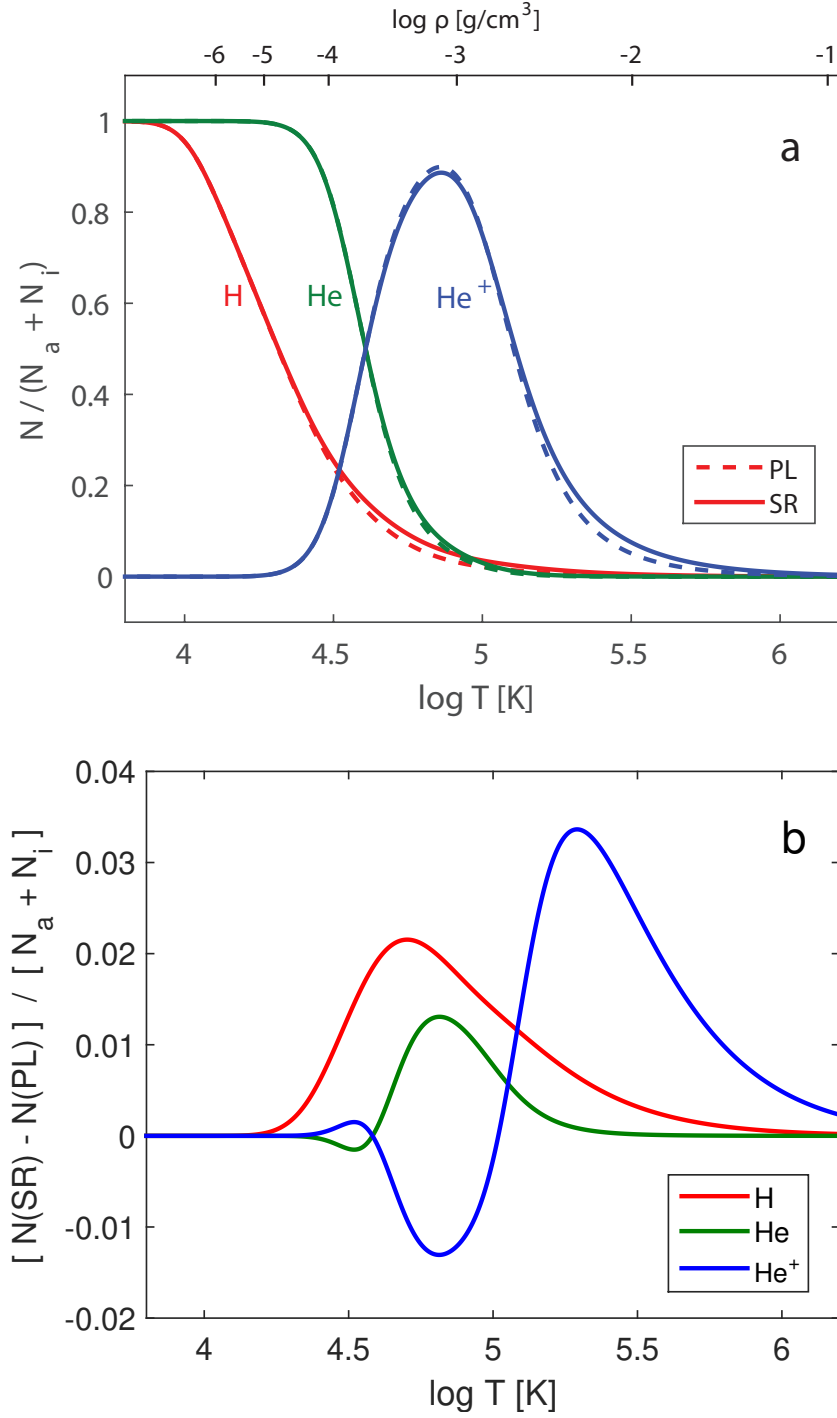


Figure 4. Hydrogen and helium ionization at the (T, ρ) points of solar model. *Red curves* are for hydrogen atom, *green* – for helium atom, and *blue* – for ion He⁺. (a) *Dashed curves* are obtained using PL partition function, *solid* – using SR partition function. (b) Difference between ionization in SR and PL approaches.

$\log T \simeq 4.8$. Because of the ionization delay, one would expect the Γ_1 (SR) profile to be shifted toward high temperatures. But this would be the case if ionization shifts uniformly over the entire region. In this case, the profile shift would lead to the fact that Γ_1 (PL) $<$ Γ_1 (SR) in the decline region, and after passing the minimum in Γ_1 , the sign of the difference would be reversed.

However, this is not the case in our comparison. Before reaching the minimum of Γ_1 there is no difference between the two cases. This is because hydrogen ionization begins at temperatures lower than that when the sum variation begins in Q (PL). That is, the description of the initial stage of ionization is the same in the PL and SR models. The differences between the models begin just in the region of the Γ_1 minimum or even at higher temperatures. Note also that the ionization of hydrogen at the Γ_1 minimum is only 20%.

In the region where there is an increase of the hydrogen sum in the SR case, ionization is delayed. As a result, in the region after the Γ_1 minimum, we have the situation Γ_1 (PL) $>$ Γ_1 (SR), which is opposite to what is expected above. In Figure 5(b) (bottom panel), this region corresponds to negative values of the difference Γ_1 (SR) $-$ Γ_1 (PL).

With further temperature increase, the pattern is reversed, and again Γ_1 (PL) $<$ Γ_1 (SR). This corresponds to the theory of isoentropic curves in the ionization regions. Let us choose points A and B for which hydrogen is neutral and fully ionized, respectively. At these points, the pressure difference between the SR and PL models is zero (see Figure 13 in Appendix E). Then we can write

$$\int_A^B \delta\Gamma_1 d \log \rho = \int_A^B d(\delta \log P) = \delta \log P|_A^B = 0. \quad (11)$$

The integral is taken along the adiabat and can be taken also by the temperature:

$$\int_A^B \delta\Gamma_1 \left. \frac{\partial \log \rho}{\partial \log T} \right|_S d \log T = \int_A^B \delta\Gamma_1 (\Gamma_3 - 1)^{-1} d \log T = 0. \quad (12)$$

Thus, a smaller Γ_1 in one region must be compensated by a region of the opposite sign. As a result, we observe a picture not just of Γ_1 displacement, but more complex deformation of the profile in the region of Γ_1 growth, in the form of winding model profiles. Amplitude of the difference between SR and PL reaches 10^{-2} . The difference between Γ_1 in SR and PL approaches does not sensitive to points (T, ρ) of a solar model. We examine this effect for several solar models in Appendix F.

In Figure 5(b), we see the deviation of the Γ_1 -difference from zero at temperatures $\log T > 5$. The reason for this, in our opinion, is the Coulomb effect. But the consideration of this effect is beyond the scope of this paper.

The same effect of Γ_1 -disturbance appears for all H-like ionizations. Figure 6 demonstrates the effect of hydrogen shifting on the position of the helium hump. With respect to the Γ_1 profile, the helium hump shifts almost isomorphically toward high temperatures in the transition from the SR to the PL model. This direction of the shift is not consistent with the shift of the ionization zones,

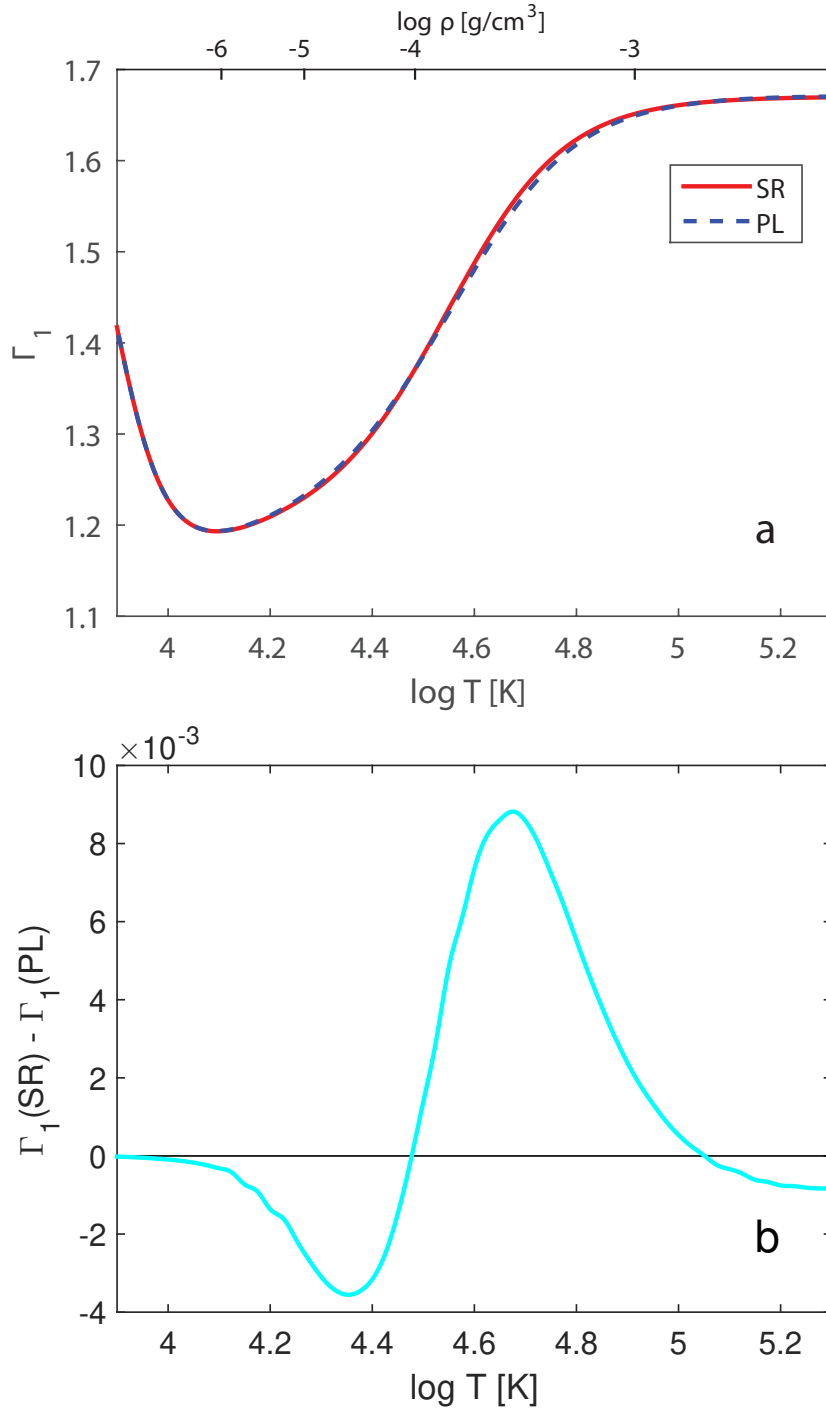


Figure 5. Γ_1 profiles in SR and PL approaches for pure hydrogen plasma (a) and difference between them (b). Γ_1 are computed at points (T, ρ) from solar model.

including the helium ionization shown in Figure 4. Helium ionization, like hydrogen, occurs at higher temperatures in the SR model. However, the shifted Γ_1 profile for a purely hydrogen plasma shows exactly the same shift in temperature as in the case of helium Γ_1 profiles.

The explanation of this effect is related to the interaction of hydrogen and helium ionizations through the number of free electrons. In the case of SR model, hydrogen ionization occurs at higher temperatures. That is, the number of free electrons is smaller than in the case of PL model. This leads to the fact that the ionization of helium is easier because the fewer free electrons, the easier it is for the corresponding ion to ionize. As a result, in the SR model, the perturbation of Γ_1 due to helium is shifted toward lower temperatures compared to the case of the PL model.

6. Conclusion

Two models of cut-off factors describing the contribution of excited states have been used to analyze a pure hydrogen plasma under solar conditions. The SR model predicts a larger contribution of bound states of hydrogen than the PL model. The main result is that in the case of the SR model, hydrogen ionization occurs deeper (at higher temperatures) than in the case of the PL-function. The proton and free electron number curves are shifted toward higher temperatures for the SR case. The shift of the ionization region is fully reflected in the pressure difference in the two models. The pressure in the SR case is always lower than in the PL case, and the SR-PL difference represents a bell-shaped depression (see Appendix E).

However, from the systematic temperature shift of ionization, two corollaries emerge.

The first one concerns the behavior of Γ_1 profiles. The perturbation of Γ_1 under the considered conditions does not lead to a simple shift of its profile in depth. In fact, the Γ_1 profiles in the two models wind up on each other. While in the region of the Γ_1 minimum the transition to the SR-function prolongs smaller Γ_1 to the region of high temperatures (ionization is delayed), the opposite effect occurs with further temperature increase. The Γ_1 in the SR-model reaches the limit values faster for a fully ionized plasma. This effect follows from the theory of adiabatic profiles, and is clearly shown on the example of pure hydrogen. As a result, the total ionization profile of Γ_1 does not shift much with the degree of ionization, but rather deforms in its (hotter) wing, becoming steeper. This effect is considered on the example of a purely hydrogen plasma.

Another consequence concerns the interaction of hydrogen and helium ionizations at solar conditions. Helium ionization occurs against the background of the ongoing incomplete ionization of hydrogen. It was found that if hydrogen ionization is delayed, helium ionization is enhanced on the contrary and occurs at lower temperatures. Conversely, easier ionization of hydrogen leads to more difficult ionization of helium.

An accurate description of the perturbation of the Γ_1 profile due to the contribution of excited states for the ionization of ions other than hydrogen and

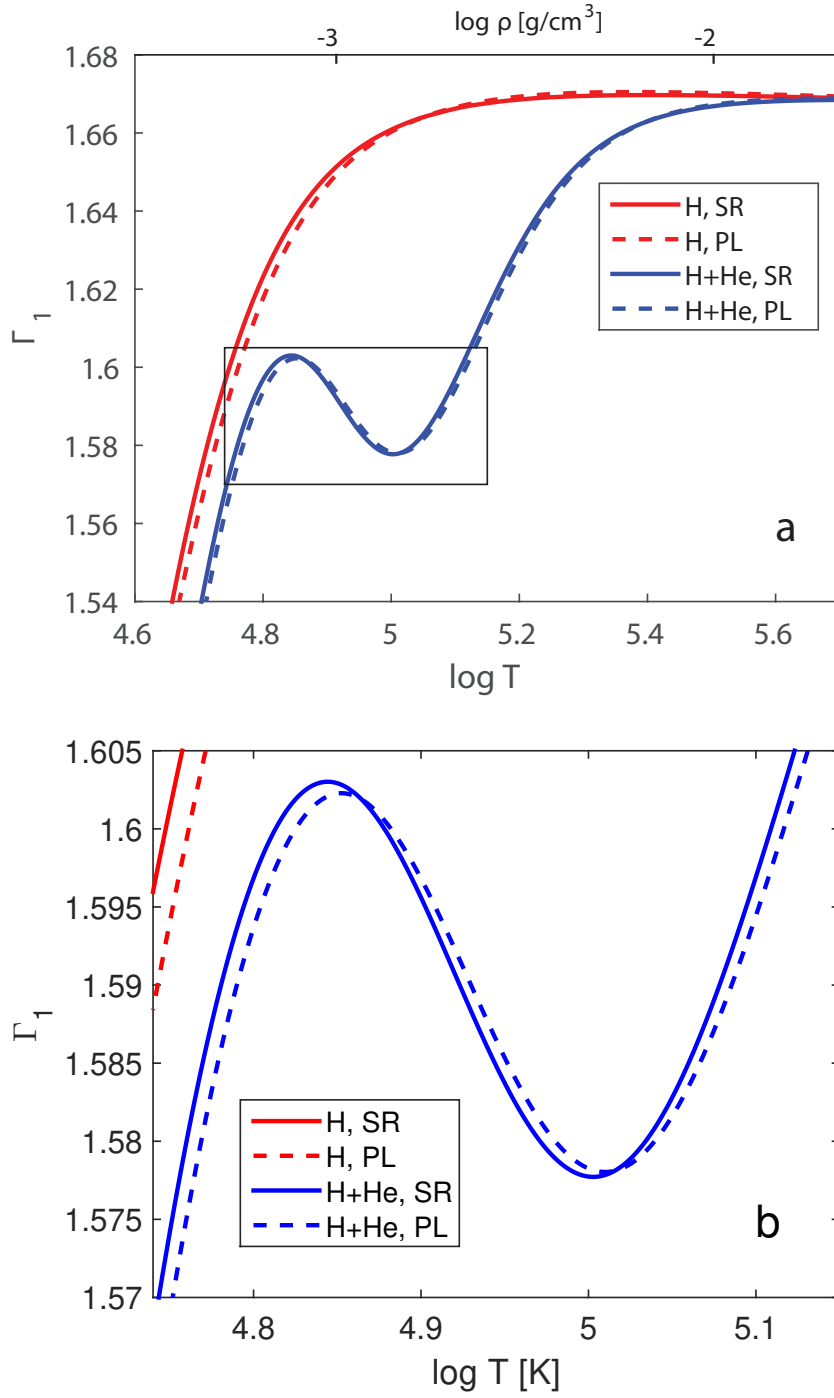


Figure 6. Γ_1 profiles in H-He plasma ($X = 0.75$, $Y = 0.25$) in SR and PL approaches at different scales (a) and (b).

helium requires further study. This is important for the method of decomposition by Z contributions (Baturin et al. 2022).

The model for cut-off factors, borrowed from the PF theory in the physical picture, is able to provide a framework for describing the ionization of hydrogen and helium at solar conditions. In the outer layers of the Sun, where hydrogen ionization process is dominant, we need enhancement of models of the hydrogen atom to improve the EOS description. The transition from one model of hydrogen ionization to another is able not only to strongly perturb the Γ_1 profile in the outer layers, but also indirectly affects the position of the helium ionization zone. Both features play a fundamental role in the inversion procedures, as well as in the construction of the seismic model of the Sun.

Appendix

A. Hydrogen Ionization in Other Equations of State

Ionization of hydrogen is different generally in various equations of state. Comparison of SAHA-S EOS with selected equations of state was performed previously by Gryaznov and Iosilevskiy (2016) along isohores. In contrast, we show comparison at the points of solar model. We examine equations of state widely used in astrophysics, i.e. OPAL (Rogers and Nayfonov 2002) and FreeEOS (Irwin 2012).

Figure 7 shows differences of Γ_1 for hydrogen plasma. FreeEOS and OPAL curves lie between SR and PL ones, closer to SR, in the region of hydrogen ionization ($\log T \sim 4 - 5$). Their maximal deviation from PL curve is about $6 \cdot 10^{-3}$. The deviations in other regions are smaller 10^{-3} .

B. Cut-off Factors and Partition Functions for Several States

Figure 8 shows the values of the weights of excited states for a fixed temperature. A sufficiently low temperature $T = 1.5 \cdot 10^4 K$ was chosen as an example. The weight factor for the ground state of hydrogen turns out to be close to unity. The values of other excited states were calculated for the same temperature using Expression (9). The ionization potentials for excited states are significantly lower than those of the ground state. Therefore, the calculation results turn out to be located at lower values of α_n , i.e. shifted to the right on the graph. The values of the weight factors of excited states quickly fall into the “cut-off” section of the weight function, even if the ground state continues to be equal to unity.

Figure 9 shows the contribution of each subsequent excited state to the sum Q compared to the sum calculated with a smaller number of states. For the SR model, the contribution of excited states is quite significant compared to the sum over the ground state, reaching 30% in the region of the maximum sum $\log T = 4.8$. Excited states in the case of PL make a noticeable contribution, but it does not exceed 10% of the ground state, and the sum itself does not exceed 1.04.

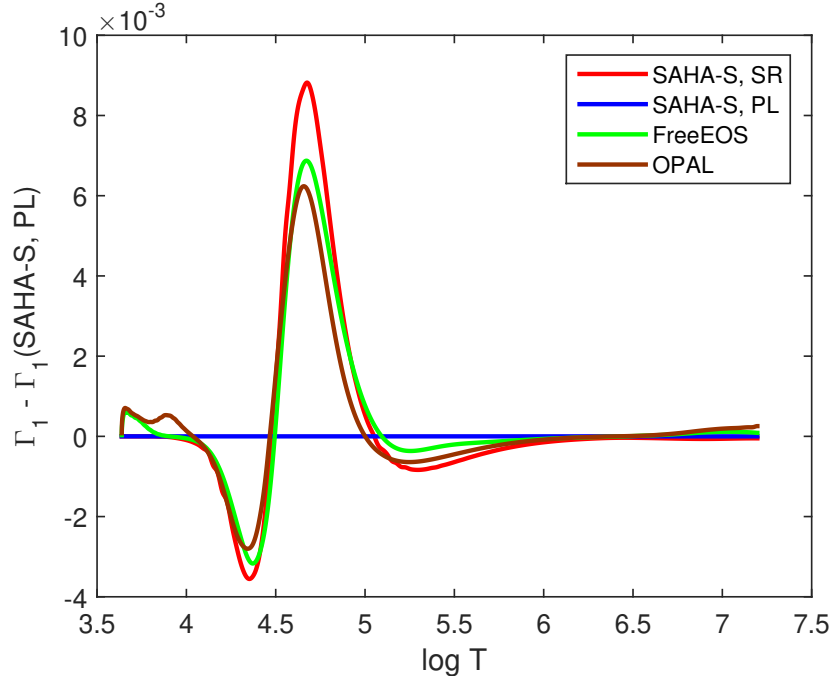


Figure 7. Deviations of Γ_1 for hydrogen plasma computed in various EOS from Γ_1 in SAHA-S with PL partition function.

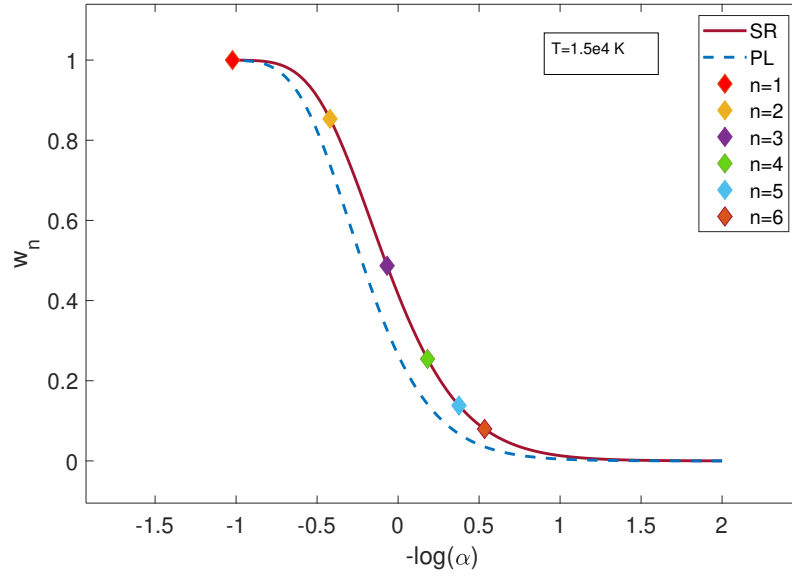


Figure 8. Cutoff factors w_n according expressions 7 and 9. An argument $\alpha = I_n/kT$, where $I_n = I_H/n^2$ is ionization energy for state n . The curves on this plot are independent of the temperature, but the values w_n depend and are shown for $T = 10^4$ K.

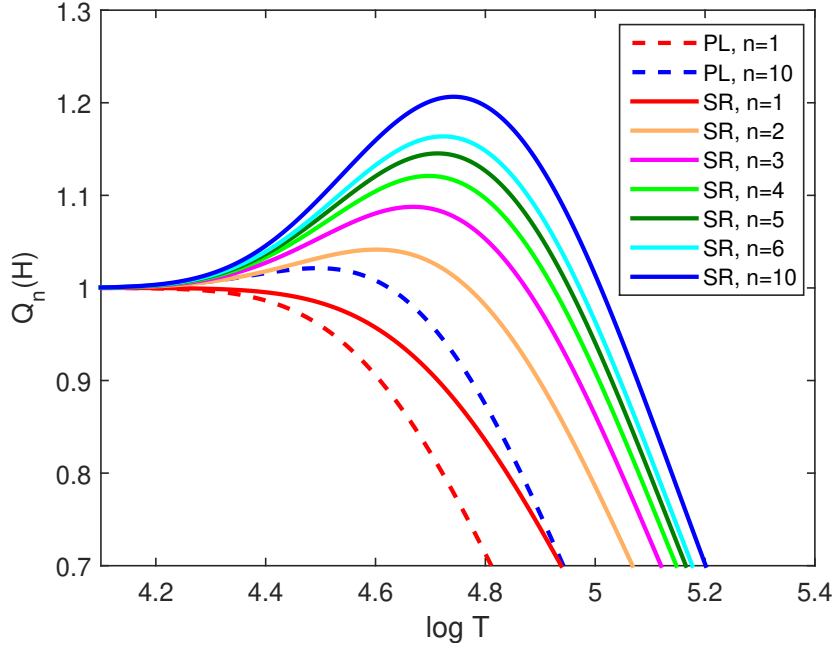


Figure 9. Partition function Q calculated for several limit numbers n .

C. Fraction of Hydrogen Atoms in the Central Part of the Sun

The fraction of neutral hydrogen below the convection zone is plotted in Figure 10 for the both cases PL and SR. A part of neutral hydrogen is small as 10^{-4} .

D. Discussion on Mott Condition

The functions PL and SR depend only on temperature and are independent of density. In this section, we consider the question of how good this approximation is under the conditions of the convective zone of the Sun. At high densities, when the average distance between atoms is smaller than their sizes, the atoms are destroyed. This condition is called the Mott condition (see, e.g., Ebeling, Kraeft, and Röpke 2012). The radius of a hydrogen atom in an excited state with number n can be estimated by the formula

$$a_n = n^2 a_B, \quad (13)$$

where a_B is the Bohr radius. This equality allows us to estimate the critical density ρ_n , above which atoms with the level n and higher do not exist:

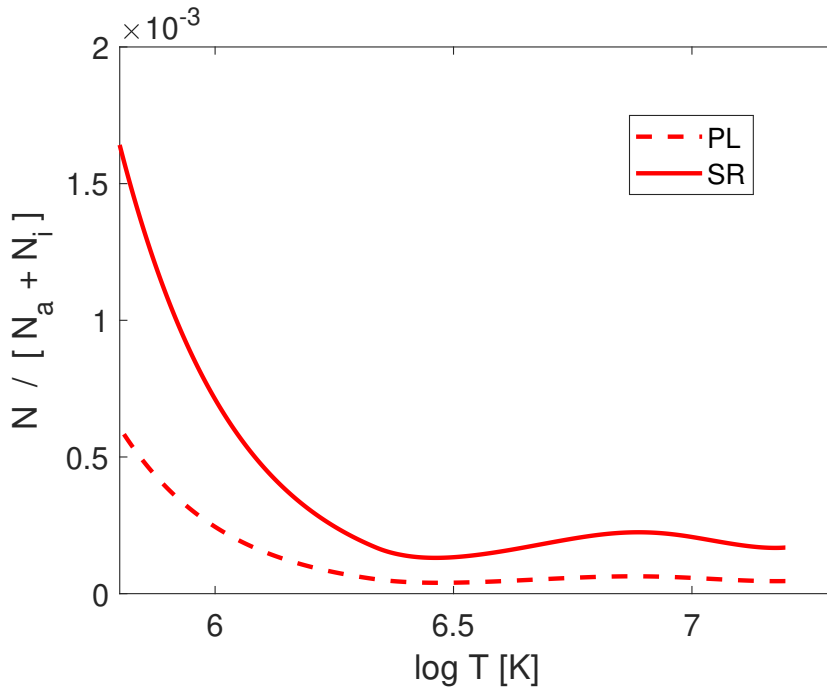


Figure 10. Fraction of hydrogen atoms in the central part of the Sun.

$$\rho_n = \frac{m_H}{(4/3)\pi a_n^3}. \quad (14)$$

Here m_H is the mass of the hydrogen atom. In Figure 11, the critical densities for n from 1 to 20 are shown by black horizontal lines. The difference between the densities ρ_n also decreases with increasing n .

This figure also shows the temperature and density in the solar model (red curve). According to the Mott condition, there are no neutral atoms at $\log T > 6.58$, they are destroyed due to the high density. At lower temperatures, $\log T = 6.45 - 6.58$, only atoms in the ground state ($n = 1$) can exist. At $\log T = 6.16 - 6.45$, atoms exist in states $n = 1$ and 2, and so on.

We calculate the partition function SR, leaving only the limited number of levels. The result is shown in Figure 12 by blue circles. Taking into account the bound states using Mott conditions does not significantly affect the value of the partition function $Q(H)$.

E. Influence of Partition Function on Pressure

Figure 13 shows pressure differences between PL and SR cases for pure hydrogen and hydrogen-helium mixture. The pressure in the SR case is always lower than in the PL. The difference between the pressures in the ionization region of hydrogen and helium reaches one percent.

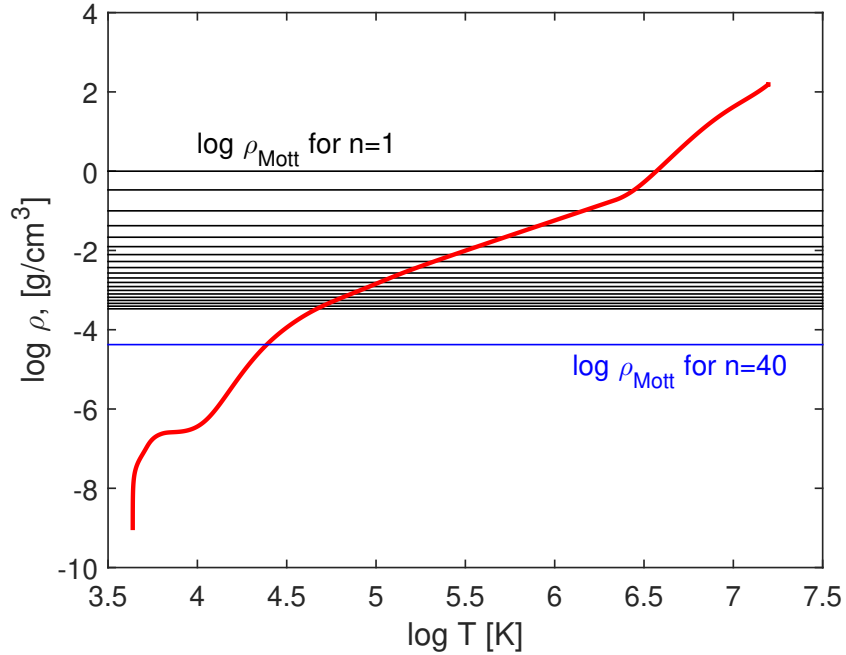


Figure 11. Densities corresponding to the Mott condition for $n = 1 - 20$ (black horizontal lines), $n = 40$ (blue line), as well as the temperature and density in the solar model (red curve).

F. Sensitivity to Solar Models

In this section, we examine if our result depends on points (T, ρ) . There are many standard and non-standard solar models in up-to-date literature (see e.g. review by Christensen-Dalsgaard 2021). Our main result is obtained for standard solar model computed with SAHA-S equation of state for high- Z solar abundances, i.e. mass fraction of elements heavier than helium is $Z = 0.018$ (Ayukov and Baturin 2017). Now we consider, as an example, a solar model computed for low- Z abundances $Z = 0.0136$ (Ayukov and Baturin 2017). We consider also Model S by Christensen-Dalsgaard et al. (1996), a high- Z model, computed with OPAL equation of state, other nuclear reactions etc.

Figure 14 shows the difference between Γ_1 for hydrogen plasma computed using SR and PL partition functions at points (T, ρ) of these three models. The curves are not distinguishable at the scale of the figure. Thus, the effect of partition function on adiabatic exponent is the same at points of various solar models.

Acknowledgments All our research is based on the enormous contribution of our colleague, friend and teacher A.N. Starostin (1940-2020) to the quantum-statistical theory of the equation of state.

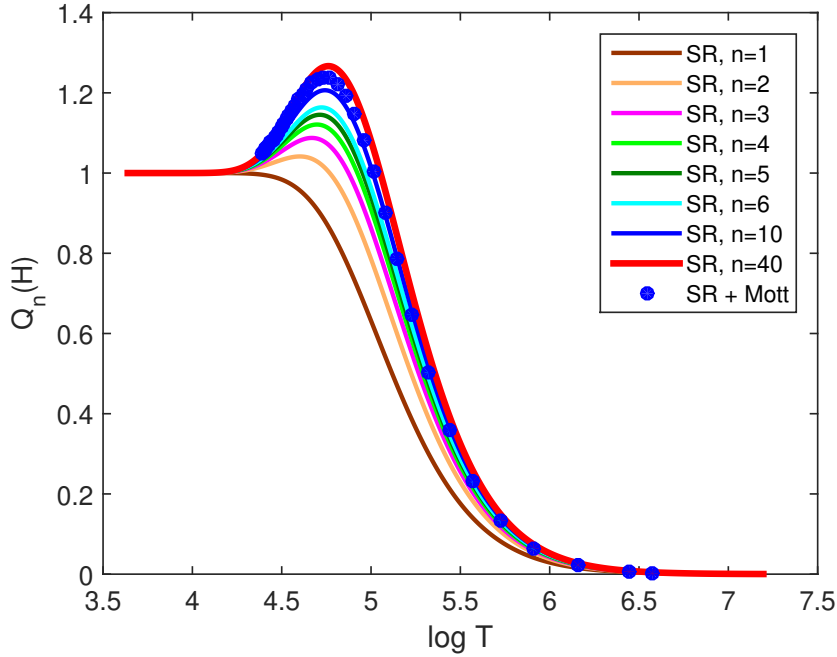


Figure 12. Partition function SR calculated for different numbers of levels (*curves*), and also taking into account the Mott condition (*blue circles*).

Author Contribution V.A.B. proposed the idea of the thorough analysis of hydrogen ionization, from the atomic partition function to the Γ_1 -behavior. The methodology of the paper, including theoretical, computational and editorial framework was performed by V.A.B. A.S.V. was responsible for thermodynamics and solar modeling computations. A.V.O. and A.B.G. provide necessary numerical and theoretical computations of the partition functions. A.V.O. is mostly involved into writing and textual preparing of the paper. V.K.G. and I.L.I. provided all necessary computations in the frames of SAHA-S EOS with PL and SR partition functions. They also provide a theoretical basis to the Starostin-Roerich partition function. W.D. provided the theoretical arguments for the combination of the chemical and physical pictures of the EOS. All the co-authors contributed to the interpretation of the results and were involved in the discussions.

Funding The study by V.K. Gryaznov is conducted under the government contract for fundamental research registration number 124020600049-8.

Data Availability No datasets were generated or analysed during the current study.

Declarations

Conflict of interest The authors declare no competing interests.

References

Ayukov, S.V., Baturin, V.A.: 2017, Helioseismic models of the sun with a low heavy element abundance. *Astron. Rep.* **61**, 901. DOI. ADS.

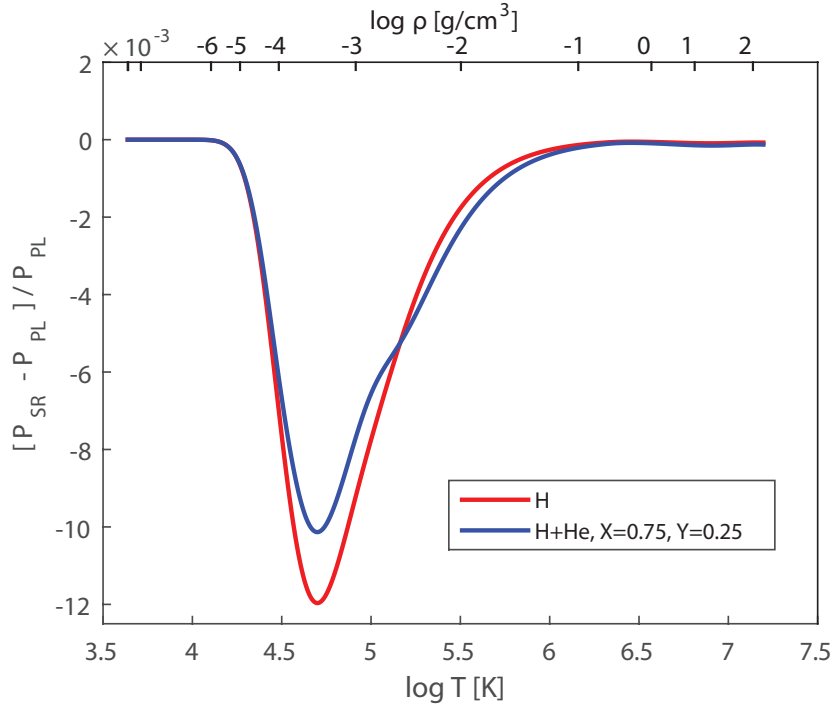


Figure 13. Difference between pressures computed in SR and PL approaches.

- Baturin, V.A., Däppen, W., Oreshina, A.V., Ayukov, S.V., Gorshkov, A.B.: 2019, Interpolation of equation-of-state data. *Astron. Astrophys.* **626**, A108. [DOI](#). [ADS](#).
- Baturin, V.A., Oreshina, A.V., Däppen, W., Ayukov, S.V., Gorshkov, A.B., Gryaznov, V.K., Iosilevskiy, I.L.: 2022, Ionization of heavy elements and the adiabatic exponent in the solar plasma. *Astron. Astrophys.* **660**, A125. [DOI](#). [ADS](#).
- Brillouin, L.: 1930, *Les Statistiques Quantiques et leurs Applications*, Presse Univ. de France.
- Chabrier, G., Debras, F.: 2021, A New Equation of State for Dense Hydrogen-Helium Mixtures. II. Taking into Account Hydrogen-Helium Interactions. *Astrophys. J.* **917**, 4. [DOI](#). [ADS](#).
- Chabrier, G., Mazevet, S., Soubiran, F.: 2019, A New Equation of State for Dense Hydrogen-Helium Mixtures. *Astrophys. J.* **872**, 51. [DOI](#). [ADS](#).
- Christensen-Dalsgaard, J.: 2021, Solar structure and evolution. *Living Rev. Solar Phys.* **18**, 2. [DOI](#). [ADS](#).
- Christensen-Dalsgaard, J., Däppen, W., Ayukov, S.V., Anderson, E.R., Antia, H.M., Basu, S., Baturin, V.A., Berthomieu, G., Chaboyer, B., Chitre, S.M., Cox, A.N., Demarque, P., Donatowicz, J., Dziembowski, W.A., Gabriel, M., Gough, D.O., Guenther, D.B., Guzik, J.A., Harvey, J.W., Hill, F., Houdek, G., Iglesias, C.A., Kosovichev, A.G., Leibacher, J.W., Morel, P., Proffitt, C.R., Provost, J., Reiter, J., Rhodes, J. E. J., Rogers, F.J., Roxburgh, I.W., Thompson, M.J., Ulrich, R.K.: 1996, The Current State of Solar Modeling. *Science* **272**, 1286. [DOI](#). [ADS](#).
- Ebeling, W.: 1969, Coulomb interaction and ionization equilibrium in partially ionized plasmas. *Physica* **43**, 293. [DOI](#). [ADS](#).
- Ebeling, W.: 2017, Max Planck and Albrecht Unsöld on plasma partition functions and lowering of ionization energy. *Contrib. Plasma Phys.* **57**, 441. [DOI](#). [ADS](#).
- Ebeling, W., Fortov, V.E., Filinov, V.: 2017, *Quantum Statistics of Dense Gases and Nonideal Plasmas*. [DOI](#). [ADS](#).
- Ebeling, W., Kraeft, W.D., Kremp, D.: 1976, *Theory of Bound States and Ionization Equilibrium in Plasmas and Solids*, Akademie-Verlag.
- Ebeling, W., Kraeft, W.-D., Röpke, G.: 2012, On the quantum statistics of bound states within

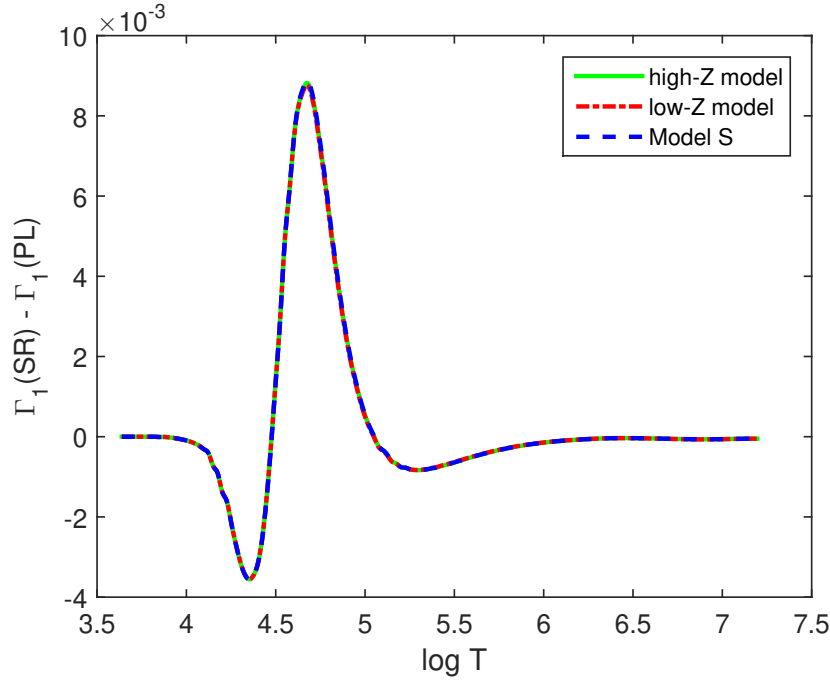


Figure 14. Difference between Γ_1 for hydrogen plasma computed using SR and PL partition functions at points (T, ρ) of various models.

- the Rutherford model of matter. *Annalen der Physik* **524**, 311. [DOI](#). [ADS](#).
- Ebeling, W., Reinholz, H., Röpke, G.: 2020, Hydrogen, helium and lithium plasmas at high pressures. *Eur. Phys. J. Spec. Top.* **229**, 3403. [DOI](#). [ADS](#).
- Ebeling, W., Reinholz, H., Röpke, G.: 2021, Equation of state of hydrogen, helium, and solar plasmas. *Contrib. Plasma Phys.* **61**, e202100085. [DOI](#). [ADS](#).
- Filinov, A.V., Bonitz, M.: 2023, Equation of state of partially ionized hydrogen and deuterium plasma revisited. *Phys. Rev. E* **108**, 055212. [DOI](#). [ADS](#).
- Graboske, H.C., Harwood, D.J., Rogers, F.J.: 1969, Thermodynamic Properties of Nonideal Gases. I. Free-Energy Minimization Method. *Physical Review* **186**, 210. [DOI](#). [ADS](#).
- Gryaznov, V.K., Iosilevskiy, I.L.: 2016, Thermodynamic Properties of Hydrogen Plasma to Megabars. *Contrib. Plasma Phys.* **56**, 352. [DOI](#). [ADS](#).
- Gryaznov, V.K., Ayukov, S.V., Baturin, V.A., Iosilevskiy, I.L., Starostin, A.N., Fortov, V.E.: 2004, SAHA-S model: Equation of State and Thermodynamic Functions of Solar Plasma. In: Celebonovic, V., Gough, D., Däppen, W. (eds.) *Equation-of-State and Phase-Transition in Models of Ordinary Astrophysical Matter*, *American Institute of Physics Conference Series* **731**, AIP, 147. [DOI](#). [ADS](#).
- Gryaznov, V.K., Ayukov, S.V., Baturin, V.A., Iosilevskiy, I.L., Starostin, A.N., Fortov, V.E.: 2006, Solar plasma: calculation of thermodynamic functions and equation of state. *J. Phys. A: Math. Gen.* **39**, 4459. [DOI](#). [ADS](#).
- Harris, G.M., Roberts, J.E., Trulio, J.G.: 1960, Equilibrium Properties of a Partially Ionized Plasma. *Phys. Rev.* **119**, 1832. [DOI](#). [ADS](#).
- Houdayer, P.S., Reese, D.R., Goupil, M.-J., Lebreton, Y.: 2021, Properties of the ionisation glitch. I. Modelling the ionisation region. *Astron. Astrophys.* **655**, A85. [DOI](#). [ADS](#).
- Irwin, A.W.: 2012, FreeEOS: Equation of State for stellar interiors calculations, Astrophysics Source Code Library, record ascl:1211.002. [ADS](#).
- Kraeft, W.D., Kremp, D., Ebeling, W., Röpke, G.: 1986, *Quantum Statistics of Charged Particle Systems*, Plenum edn..

- Krasnikov, Y.G.: 1968, Concerning the Thermodynamics of a Dense Plasma. *J. Exp. Theor. Phys.* **26**, 1252.
- Larkin, A.I.: 1960, Thermodynamic Functions of a Low-Temperature Plasma. *J. Exp. Theor. Phys.* **11**, 1363.
- Mihalas, D., Däppen, W., Hummer, D.G.: 1988, The equation of state for stellar envelopes. II - Algorithm and selected results. *Astrophys. J.* **331**, 815. DOI. ADS.
- Militzer, B., Ceperley, D.M.: 2001, Path integral Monte Carlo simulation of the low-density hydrogen plasma. *Phys. Rev. E* **63**, 066404. DOI. ADS.
- Militzer, B., Hubbard, W.B.: 2013, Ab Initio Equation of State for Hydrogen-Helium Mixtures with Recalibration of the Giant-planet Mass-Radius Relation. *Astrophys. J.* **774**, 148. DOI. ADS.
- Planck, M.: 1924, Zur Quantenstatistik des Bohrschen Atommodells. *Annalen der Physik* **380**, 673. DOI. ADS.
- Potekhin, A.Y.: 1996, Ionization equilibrium of hot hydrogen plasma. *Phys. Plasmas* **3**, 4156. DOI. ADS.
- Pradhan, A.K.: 2024, Interface of equation of state, atomic data, and opacities in the solar problem. *Mon. Not. R. Astron. Soc.* **527**, L179. DOI. ADS.
- Prigogine, I., Defay, R.: 1954, *Chemical Thermodynamics*, Longmans green and co edn..
- Rogers, F.J.: 1986, Occupation Numbers for Reacting Plasmas: The Role of the Planck-Larkin Partition Function. *Astrophys. J.* **310**, 723. DOI. ADS.
- Rogers, F.J., Nayfonov, A.: 2002, Updated and Expanded OPAL Equation-of-State Tables: Implications for Helioseismology. *Astrophys. J.* **576**, 1064. DOI. ADS.
- Rogers, F.J., Swenson, F.J., Iglesias, C.A.: 1996, OPAL Equation-of-State Tables for Astrophysical Applications. *Astrophys. J.* **456**, 902. DOI. ADS.
- Saha, M.N.: 1921, On a Physical Theory of Stellar Spectra. *Philos. Trans. Royal Soc. A* **99**, 135. DOI. ADS.
- Starostin, A.N., Roerich, V.C.: 2004, Corrected EOS of Weakly-Nonideal Hydrogen Plasmas without Mysteries. In: Celebonovic, V., Gough, D., Däppen, W. (eds.) *Equation-of-State and Phase-Transition in Models of Ordinary Astrophysical Matter*, American Institute of Physics Conference Series **731**, 83. DOI. ADS.
- Starostin, A.N., Roerich, V.C.: 2006, Equation of state of weakly nonideal plasmas and electroneutrality condition. *J. Phys. A: Math. Gen.* **39**, 4431. DOI. ADS.
- Starostin, A.N., Roerich, V.C., More, R.M.: 2003, How correct is the EOS of weakly nonideal hydrogen plasmas? *Contrib. Plasma Phys.* **43**, 369. DOI. ADS.
- Starostin, A.N., Roerich, V.C., Gryaznov, V.K., Fortov, V.E., Iosilevskiy, I.L.: 2009, The influence of electron degeneracy on the contribution of bound states to the non-ideal hydrogen plasma EOS. *J. Phys. A: Math. Gen.* **42**, 214009. DOI. ADS.
- Vedenov, A.A., Larkin, A.I.: 1959, *J. Exp. Theor. Phys.* **9**, 806.
- Wendland, D., Ballenegger, V., Alastuey, A.: 2014, Quantum partition functions of composite particles in a hydrogen-helium plasma via path integral Monte Carlo. *J Chem Phys* **141**, 184109. DOI. ADS.